

# Electron probe X-ray microanalysis of cisplatin-induced cell death in rat pheochromocytoma PC12 cells

Juan M. Ramos<sup>1</sup>, Francisco Arrebola<sup>1,2</sup>, Francisco J. Fernández-Cervilla<sup>2,3</sup>,  
Vicente Crespo<sup>1</sup> and Eduardo Fernández-Segura<sup>1,2</sup>

<sup>1</sup>Department of Histology, Faculty of Medicine, University of Granada, Granada, Spain, <sup>2</sup>Institute of Neurosciences F. Olóriz, Centro de Investigaciones Biomédicas (CIBM), Campus de la Salud, Armilla, Granada, Spain and <sup>3</sup>Department of Otorhinolaryngology, Faculty of Medicine, University of Granada, Granada, Spain

**Summary.** Several lines of evidence suggest that cisplatin-induced cell death is not always the result of apoptosis. A distinctive feature between apoptosis and necrosis is the alteration in cell volume regulation and ion homeostasis. Here we analyzed the changes in intracellular element content during cell death induced by exposure to therapeutic concentrations of cisplatin in the PC12 cell line. To quantitate Na, Cl and K content, electron probe X-ray microanalysis (EPXMA) was performed in whole freeze-dried cells. We also traced the alterations in morphological features with fluorescence and transmission electron microscopy. EPXMA demonstrated progressive derangement of the absolute intracellular Na, Cl and K contents. Cisplatin-treated cells showed two microanalytical patterns: 1) cells with alterations in elemental content typical of apoptosis, i.e., an increase in intracellular Na and a decrease in intracellular Cl and K, and 2) cells characterized by an increase in Na content and a decrease in K content, with no changes in Cl content. This intracellular profile for Na, Cl, and K was not typical of necrosis or apoptosis. Morphological analysis revealed two cellular phenotypes: 1) cells characterized by a phenotype typical of apoptosis, and 2) cells characterized by a hybrid phenotype combining variable features of apoptosis and necrosis. Taken together, our findings suggest that therapeutic concentrations of cisplatin may cause a hybrid type of cell death characterized by concurrent apoptosis and necrosis in the same individual PC12 cell.

**Key words:** PC12 cell, Cisplatin, X-ray microanalysis, Apoptosis, Necrosis, Hybrid cell death, Potassium, Sodium, Chlorine

## Introduction

Apoptosis and necrosis are the two basic modes of cell death purportedly defined by different biochemical, morphological and functional characteristics. A fundamental feature that distinguishes apoptosis from necrosis is the alteration in cell volume. Cell shrinkage during apoptosis, which occurs under normotonic conditions (apoptotic volume decrease, AVD), has been associated with regulatory volume decrease, since the loss of volume after apoptotic stimuli is related to the activation of K<sup>+</sup> and Cl<sup>-</sup> channels (Maeno et al., 2000, 2006; Okada et al., 2001). By analogy, necrotic volume increase (NVI) has been proposed to denote the active nature of the prelethal phase of necrosis, which involves water influx driven by NaCl influx, a mechanism similar to the one involved in regulatory volume increase induced by osmotic cell shrinkage (Barros et al., 2001).

Previous studies have characterized the sequence of changes in Na, Cl and K content in relation to morphological and molecular features in cells undergoing necrosis (Buja et al., 1985; Jones et al., 1989; Thandroyen et al., 1992) or apoptosis (Fernández-Segura et al., 1999; Skepper et al., 1999; Salido et al., 2001, 2002; Arrebola et al., 2006). To evaluate intracellular elemental composition, these studies used electron probe X-ray microanalysis (EPXMA). This method is an analytical electron microscope technique that makes it possible to identify, localize, and quantify elements both at the whole cell and the intracellular level, based on the analysis of element-specific X-rays generated by the electron beam in an electron microscope (Fernández-Segura and Warley, 2008). In addition, although EPXMA measures total (bound and ionized) element content, these findings are a useful complement to the results obtained with fluorescent ion-binding dyes (Andersson and Roomans, 2002).

The mechanism of cell injury induced by cisplatin,

one of the most effective chemotherapeutic agents for the treatment of several human cancers, is not clear. Although most studies have shown that cisplatin causes apoptosis (Gill and Windebank, 1998; Fischer et al., 2001; González et al., 2001), different lines of evidence suggest that cisplatin-induced cell death is not always the result of apoptosis (Pestell et al., 2000; Gonzalez et al., 2001; Spano et al., 2008). Different studies support the possibility that some stimuli may trigger the coexistence of features of necrosis and apoptosis in the same cell (Xiao et al., 2002). This intermediate type of cell death has been designated necrapoptosis (Lemaster, 1999), aponecrosis (Formigli et al., 2000), paraptosis (Sperandio et al., 2000) or hybrid cell death (Xiao et al., 2002; Wang et al., 2003).

Taken together, these findings suggest that intermediate types of cell death may involve a combination of ionic mechanism responsible for AVD and NVI. However, limited information is available on the underlying changes in intermediate mechanisms of cell death.

Based on these premises, we decided to use EPXMA to evaluate the changes in intracellular elemental composition—mainly Na, Cl and K content—in rat pheochromocytoma PC12 cells. In addition, we also correlated these changes in elemental composition with the alterations in ultrastructural features induced by cisplatin, since transmission electron microscopy has been considered the gold standard for cell death research (Krysko et al., 2008).

## Material and Methods

### Material

*Cis*-diamine-dichloroplatinum (II) (cisplatin) was obtained from Chiesi España S.A. (Barcelona, Spain). RPMI 1640 medium, fetal bovine serum (FBS), horse serum (HS), 0.4% trypan blue solution, propidium iodide (PI), phosphate buffered saline, and polycarbonate tissue culture plate well inserts were purchased from Sigma-Química (Madrid, Spain). Glutaraldehyde and dimethylsulfoxide were from Merck (Darmstadt, Germany). Hoescht 33342 was from Molecular Probes (Leiden, Holland), and tetrazolium salt WST-1 was from Roche (Barcelona, Spain).

### Cell culture and cisplatin treatment

Rat pheochromocytoma PC12 cells were purchased from the European Collection of Animal Cell Cultures (Porto Down, U.K.). Cells were cultured in RPMI 1640 medium plus 10% heat-inactivated HS, 5% heat-inactivated FBS, 2 mM L-glutamine, and 26.7 ml/l NaHCO<sub>3</sub> without antibiotics, and were maintained at 37°C in a humidified atmosphere containing 5% CO<sub>2</sub>. For cisplatin treatment, PC12 cells (5x10<sup>5</sup> cells/ml) were incubated with a therapeutic concentration of cisplatin

(3.5 µg/ml) according to Gill and Windebank (1998) for 14, 24 and 48 h at 37°C.

### Cell viability and proliferation assays

Cell viability was assessed with the trypan blue exclusion assay. This method measures integrity of the plasma membrane as a viability parameter. For the trypan blue test, cells (5x10<sup>5</sup> cells/ml) were diluted at a ratio of 1:1 with 0.4% trypan blue solution and incubated for 5–10 min at room temperature. The loss of cell viability was estimated by counting the number of blue cells with a hemocytometer under a light microscope.

Cell proliferation was assessed with the water-soluble WST-1 reagent according to the manufacturer's instructions. This colorimetric assay is based on the cleavage of tetrazolium salts WST-1 into formazan salts by mitochondrial dehydrogenase in live cells. Briefly, PC12 cells were seeded in 96-well tissue culture plates at a density of 5x10<sup>5</sup> cells/well and exposed to cisplatin. After treatment for 14, 24, and 48 h, 10 µl WST-1 was added to each well and incubated for 2 h at 37°C. Absorbance of the formazan product was determined at 450 nm in an ELx 800 universal microplate reader (Bio-Tek Instruments, VT). Absorbance readings were normalized against control wells with medium alone.

### X-ray microanalysis

Preparation of whole cells for X-ray microanalysis was described in detail elsewhere (Fernández-Segura and Warely, 2008). Briefly, cells were removed from the culture medium and centrifuged into polycarbonate tissue culture plate well inserts (Millicell-PCF), and washed with ice-cold distilled water for 5 s to remove the culture medium. After washing, cells were plunge-frozen in liquid nitrogen and freeze-dried (Emitech K755 freeze-drier, Watford, UK) using three 1-h steps at -100°C, -70°C, and -50°C. Samples were fixed to adhesive graphite lamina on stubs and coated with carbon in a high-vacuum coating system (Emitech, Watford, UK).

X-ray microanalysis was performed in a Philips XL30 scanning electron microscope (Philips, Eindhoven, Netherlands) equipped with a Compact Detector Unit (EDAX Europe, Tilburg, Netherlands). The analytical conditions were: tilt angle 35°, take-off-angle 61.34°, and working distance 10 mm. X-ray spectra were acquired at an accelerating voltage of 10 kV with a beam current of 1 nA, and collected in the static spot mode for 200 s live time. Only one spectrum was acquired from each cell. Quantitative analysis was performed by determining the ratio (P/B) of the characteristic intensity (peak, P) to the background intensity (B) in the same energy range as the peak and comparing this P/B ratio with that obtained by analysis of a standard (Warley, 1997). The concentration of

element  $x$  in the specimen ( $Cx_{sp}$ ) was calculated according to the formula:

$$C_{x_{sp}} = \frac{(P_x/B_x)_{sp}}{(P_x/B_x)_{std}} \cdot \frac{G_{sp}}{G_{std}} \cdot C_{x_{std}}$$

where  $Cx$  is the concentration of element  $x$  in millimoles per kilogram,  $(P_x/B_x)$  is the peak-to-background ratio for the element  $x$ , the subscripts  $sp$  and  $std$  refer to specimen and standard, respectively, and  $G$  is the mean value of the atomic number squared ( $Z^2$ ) and divided by atomic weight ( $A$ ) in the sample. The standards consisted of known concentrations of mineral salts in a 20% dextran matrix, frozen and freeze-dried to resemble the specimen in its physical and chemical properties. No correction for extraneous contributions to the spectrum was applied.

#### Assessment of cell death

To evaluate the mechanism of cell death of cisplatin-treated PC12 cells, we used two complementary approaches: 1) fluorescence microscopy, and 2) transmission EM. For fluorescence microscopy, control PC12 or cisplatin-treated PC12 cells were double-stained with Hoechst 33342 (5  $\mu\text{g}/\text{ml}$ ) and PI (1  $\mu\text{g}/\text{ml}$ ) for 5 min at 37°C. Cells were observed with a Leitz Laborlux 12 microscope (Leica, Barcelona, Spain) equipped for epifluorescence illumination. Hoechst 33342 staining was evaluated with an excitation wavelength of 355-425 nm and a longpass filter of 470 for emission. For PI staining we used an excitation wavelength of 450-490 nm and a longpass filter of 515 for emission. Fluorescence images were acquired with a Leica DC100 digital camera (Leica, Barcelona, Spain), and images were processed with Adobe PhotoDeLuxe software (Adobe System, San José, CA). Cells were classified into four categories according to the degree of nuclear staining with DNA-binding Hoechst fluorochrome and their capacity to exclude PI. Type I cells showed normal uncondensed chromatin stained by Hoechst 33342 but unstained by PI; type II cells had condensed chromatin and intense staining with Hoechst 33342 but no staining with PI; type III cells were characterized by condensed chromatin and intense staining with PI; and type IV cells showed uncondensed chromatin and intense staining with PI.

For transmission EM, cells were fixed with 2% glutaraldehyde in 0.1 M phosphate buffer, pH 7.2, at 4°C for 4 h at different times after exposure to cisplatin. After fixation, samples were postfixed with 1% osmium tetroxide in 0.1 M phosphate buffer, pH 7.2, dehydrated in a graded series of acetones, embedded in Epoxy resin, sectioned with a Reichert ultramicrotome, and stained with uranyl acetate and lead citrate. Samples were viewed in a Zeiss EM902 (Zeiss, Oberkochen, Germany) transmission electron microscope.

#### Statistical analysis

Data were expressed as the mean  $\pm$  standard error of the mean. The method of Kolmogorov-Smirnov was used to test normality of the data. To compare control and experimental groups we used the Kruskal-Wallis test followed by Dunn's test. To compare two experimental groups we used the Mann-Whitney test.  $P$  values less than 0.05 were considered statistically significant. All statistical analyses were done with the GraphPad InStat 3.00 program for Windows (GraphPad Software, San Diego, CA).

## Results

#### Effect of cisplatin on cell viability and proliferation

We first examined the effects of cisplatin on the viability of PC12 cells. Figure 1A shows the changes with time in the percentage of cell survival measured as trypan blue exclusion, relative to the control value. Exposure to 3.5  $\mu\text{g}/\text{ml}$  cisplatin resulted in a time-dependent decrease in cell viability; the decrease was statistically significant after 24 h of exposure. Cisplatin also decreased cell proliferation according to the salt tetrazolium WST-1 assay (Fig. 1B). In contrast, untreated control PC12 cells showed a time-dependent increase in absorbance after all three periods of exposure to cisplatin.

#### X-ray microanalysis of cisplatin-treated PC12 cells

We initially examined cell shape in whole, freeze-dried PC12 cells. Figure 2 shows scanning electron micrographs of cisplatin-treated PC12 cells (Fig. 2A). Examination of cells treated with cisplatin for 24 and 48 h revealed essentially two distinct phenotypes: 1) round cells with a smooth surface similar to control cells, and 2) larger cells with an irregular surface and lacking the plasma membrane. Figure 2B shows representative X-ray spectra from control cells and both phenotypes of cisplatin-treated cells. The spectra from control PC12 cell showed high P and K peaks, small peaks for Na, and moderate Cl peaks. In contrast, X-ray spectra from cells with phenotype type 1 showed high Na and P peaks, moderate peaks for Cl and small K peaks. Cells with extensive structural damage -phenotype type 2- were characterized by small peaks for Na and P, and undetectable peaks for S, Cl and K.

Quantitative data for Na, Cl, K, Mg, P, and S content are shown in Figure 3. The quantitative analyses were performed only in untreated, control cells and cisplatin-treated cells with morphological phenotype type 1, since it was not relevant to investigate changes in elemental composition in cells with extensive structural damage. Untreated control PC12 cells showed the expected pattern of intracellular element content, with low Na, moderate Cl, and high K. Cells treated with cisplatin for

14 h showed no significant changes in comparison to control cells. After 24 h of exposure to cisplatin, Na increased significantly from  $55.1 \pm 2.1$  to  $85.2 \pm 8$  mmol/kg dry weight ( $P < 0.01$ ), and nonsignificant differences were found for Cl and K content. After 48 h of treatment, cells showed a significant increase in Na ( $91.2 \pm 9.3$  mmol/kg dry weight,  $P < 0.05$ ), while conversely, K decreased from  $317.5 \pm 6$  to  $254 \pm 11$  mmol/kg dry weight,  $P < 0.01$ . After 48 h there were no significant differences in intracellular Cl content between control and treated cells. Phosphorus content increased after 24 h of treatment but decreased after 48

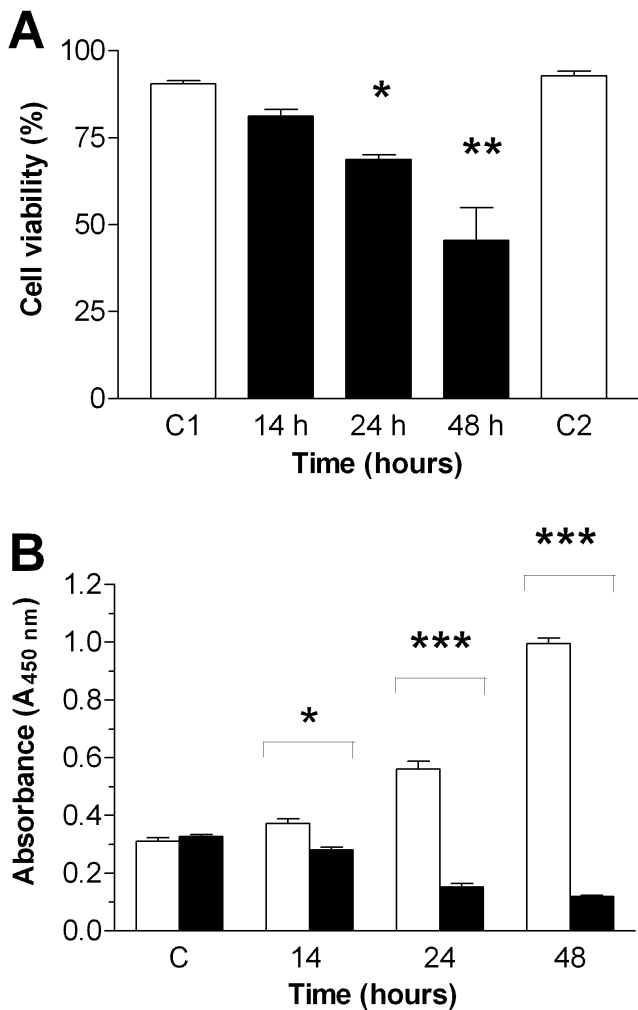


**Fig. 1.** Effects of cisplatin on cell viability (**A**) and proliferation (**B**) in PC12 cells. Cells were exposed to cisplatin for 14, 24 and 48 h. **A.** Cell viability was assessed by trypan blue exclusion, and values are expressed as percentages of the control value. Data shown are the means  $\pm$  SEM from five independent experiments (\*  $P < 0.05$ ; \*\*  $P < 0.01$ ). **B.** Cell proliferation was tested with the tetrazolium salt WST-1 assay. Values are expressed as relative absorbance of WST-1 formazan. C1, control cells in complete RPMI medium; C2, control cells incubated for 48 h in complete RPMI 1640 medium without cisplatin. Data are presented as the mean absorbance  $\pm$  SEM from two independent experiments (\*  $P < 0.05$ ; \*\*\*  $P < 0.001$ ).

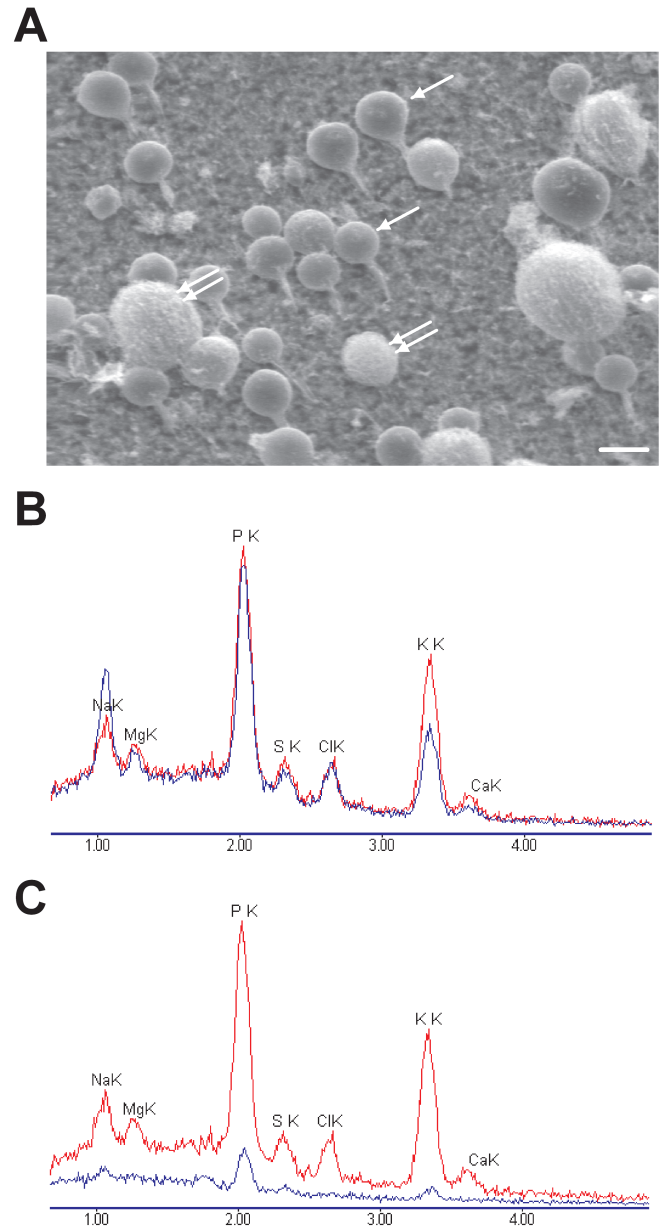


**Figure 2.** Scanning electron micrograph (**A**) and X-ray spectra (**B, C**) of whole, freeze-dried cisplatin-treated PC12 cells. Cells were washed with distilled water, cryofixed with liquid nitrogen, freeze-dried and observed with a scanning electron microscope in secondary electron mode. X-ray spectra were acquired in a Philips XL30 scanning electron microscope with a Compact Detector Unit (EDAX) at 10 kV, 1 nA beam current, and 200 s live time. **A.** Cells treated for 24 h with cisplatin were round and had a smooth surface similar to control cells (arrow), or had an irregular surface with structural damage to the plasma membrane (double arrow). Scale bar: 10  $\mu$ m. **B.** X-ray spectra of untreated, control (red line) and cisplatin-treated PC12 cells with a smooth surface -phenotype type 1- (blue line). **C.** X-ray spectra of untreated, control (red line) and cisplatin-treated PC12 cells lacking the plasma membrane -phenotype type 2- (blue line). Note that X-ray spectra from cisplatin-treated cells with a round shape and smooth surface showed high Na and P peaks, moderate peaks for Cl, and small K peak in comparison to untreated, control PC12 cells. X-ray spectra from cells with extensive structural damage showed small Na and P peaks.

## EPXMA of cisplatin-induced cell death

h, although neither of the changes was statistically significant in comparison to untreated control cells. No significant differences were found for Mg and S content.

Electron probe microanalysis data were analyzed further on a cell-by-cell basis to determine the percentages of individual PC12 cells with abnormal elemental values (Table 1). For each element (Na, Cl, and K) in the whole cell, the range of normal values was defined as two standard deviations from the mean value in the control group. Values were considered abnormal if they were outside the upper or lower limits for each element in the direction of the change expected as a result of cell injury (Jones et al., 1989). We found that 18% of the cisplatin-treated cells showed increased Na content after 24 h, and 33% showed increased Na after 48 h. Decreases in the K content were found in 18% of the cells after 24 h, and in 20% after 48 h.

However, the intracellular Cl content showed a distinctive behavior. After 24 h of exposure to cisplatin, values two standard deviations below the mean for the control group were found in approximately 9% of the cells. In contrast, after 48 h of treatment, the Cl content was more than two standard deviations above the mean control value in approximately 4.5% of the cells.

### Effect of cisplatin on morphological features

The effect of cisplatin on morphological features

was examined with fluorescence and transmission electron microscopy. For fluorescence microscopy, unfixed PC12 cells were double-stained with Hoechst 33342 and PI. Figure 4 shows representative images of PC12 cells treated with cisplatin and stained with Hoechst and PI. Figure 4B shows the time-dependent effect in each cell type during treatment with cisplatin. Cisplatin significantly decreased ( $P < 0.001$ ) the percentage of type I (viable) cells after all three periods of exposure. In untreated control PC12 cells, the percentage of morphological type I cells remained unchanged after different periods of exposure. Cell types

**Table 1.** Percentages of individual PC12 cells with abnormal values of Na, Cl and K after treatment with cisplatin<sup>1</sup>.

Time	Na		Cl		K	
	% cells below <sup>2</sup>	% cells above	% cells below	% cells above	% cells below	% cells above
14 h	-	4.4	-	2.2	-	-
24 h	-	17.8	8.9	-	17.8	-
48 h	-	33.3	-	4.4	20.0	-

<sup>1</sup>: Data are reported as mean of three independent experiments (45 measurements); <sup>2</sup>: For each element in the whole cell, the range of normal values was defined as two standard deviation from the mean in the control group.

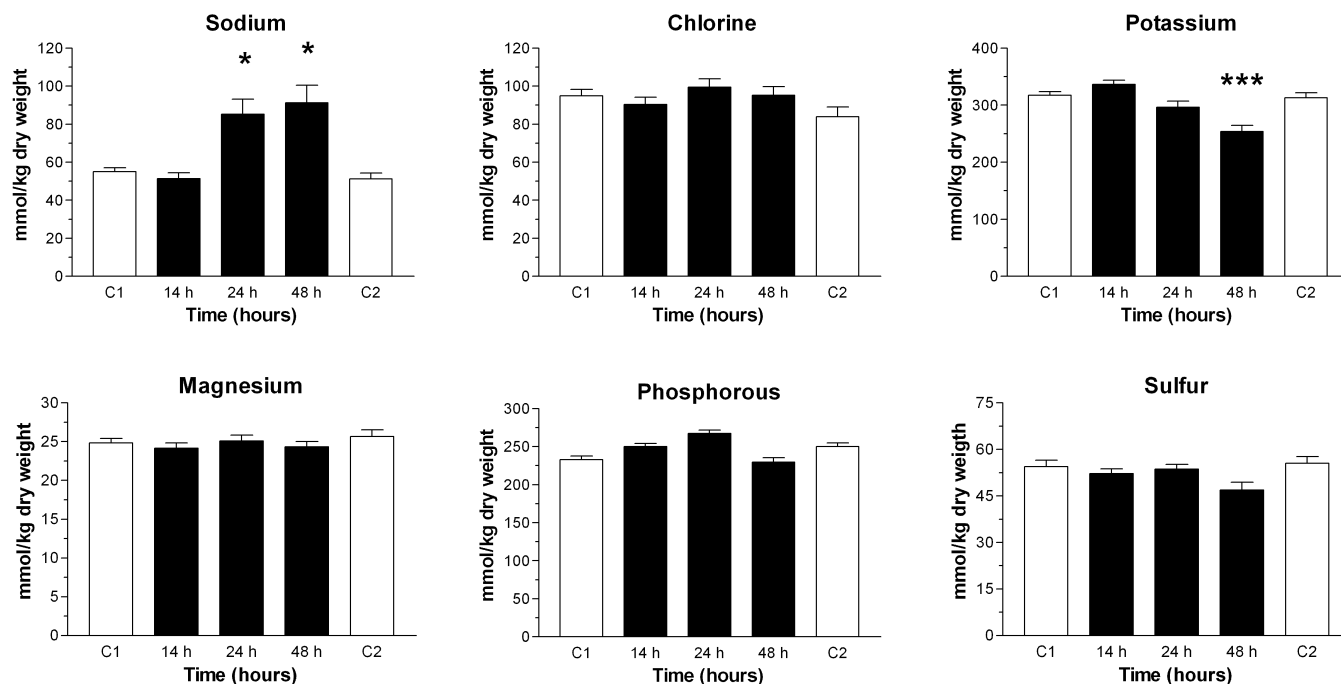


**Fig. 3.** Effects of cisplatin on sodium (Na), chlorine (Cl), potassium (K), magnesium (Mg), phosphorous (P), and sulfur (S) content in PC12 cells as determined with electron probe X-ray microanalysis. Cells were cryoprepared as indicated in the legend to Figure 2. Data are given in mmol/kg dry weight as the mean  $\pm$  SEM of three independent experiments (number of cells analyzed = 45). Significant differences between control and treated groups are indicated by asterisks (\*  $P < 0.05$ , \*\*\*  $P < 0.001$ ).

II and III were observed only in cultures of treated cells, and the differences in comparison to control cells became significant after 24 h of treatment with cisplatin. The percentage of type II cells remained constant after this time (6% at 24 h and 5% at 48 h). However, the proportion of type III cells increased significantly after 24 h of culture, and reached 50% after 48 h of treatment. The percentage of type IV cells remained unchanged, with no significant differences between untreated control and cisplatin-treated cell cultures.

We also used transmission electron microscopy to accurately characterize the mode of cell death induced by cisplatin in PC12 cells. Figure 5 shows the time-course of ultrastructural changes in cells incubated with cisplatin for 14, 24 and 48 h. Cells treated for 14 h showed no ultrastructural alterations compared to untreated control cells. After 24 h, two morphological phenotypes were found: 1) a phenotype characterized by morphological features similar to those of untreated control cells, and 2) a phenotype characterized by typical features of apoptosis such as decreased cell size, cytoplasmic condensation, and margination of the condensed chromatin to the nuclear periphery. Nuclear fragmentation and apoptotic bodies were occasionally seen. After 48 h of exposure to cisplatin, most injured cells were characterized by a variable intermediate

phenotype combining features of apoptosis and necrosis. Ultrastructural analysis revealed cells characterized by an intact nucleus with chromatin aggregated beneath the nuclear envelope, accompanied by undamaged but swollen cytoplasm surrounded by an intact plasma membrane. We also identified cells characterized by condensed nuclei with aggregated chromatin accompanied by degenerated electron-lucent residual cytoplasm, surrounded by a disrupted plasma membrane.

## Discussion

We used EPXMA on freeze-dried whole cells in a scanning electron microscope to examine the changes in intracellular composition during cell death induced by therapeutic concentrations of cisplatin in rat pheochromocytoma PC12 cells. Our microanalytical study revealed that cisplatin induced a distinctive intracellular profile for sodium (Na), chlorine (Cl), and potassium (K) which was not typical of necrosis or apoptosis. PC12 cells treated with cisplatin were characterized by an increase in intracellular Na and a decrease in intracellular K, while chlorine (Cl) showed no change after cisplatin treatment.

The increase in Na and decrease in K content reported in this study are consistent with other studies

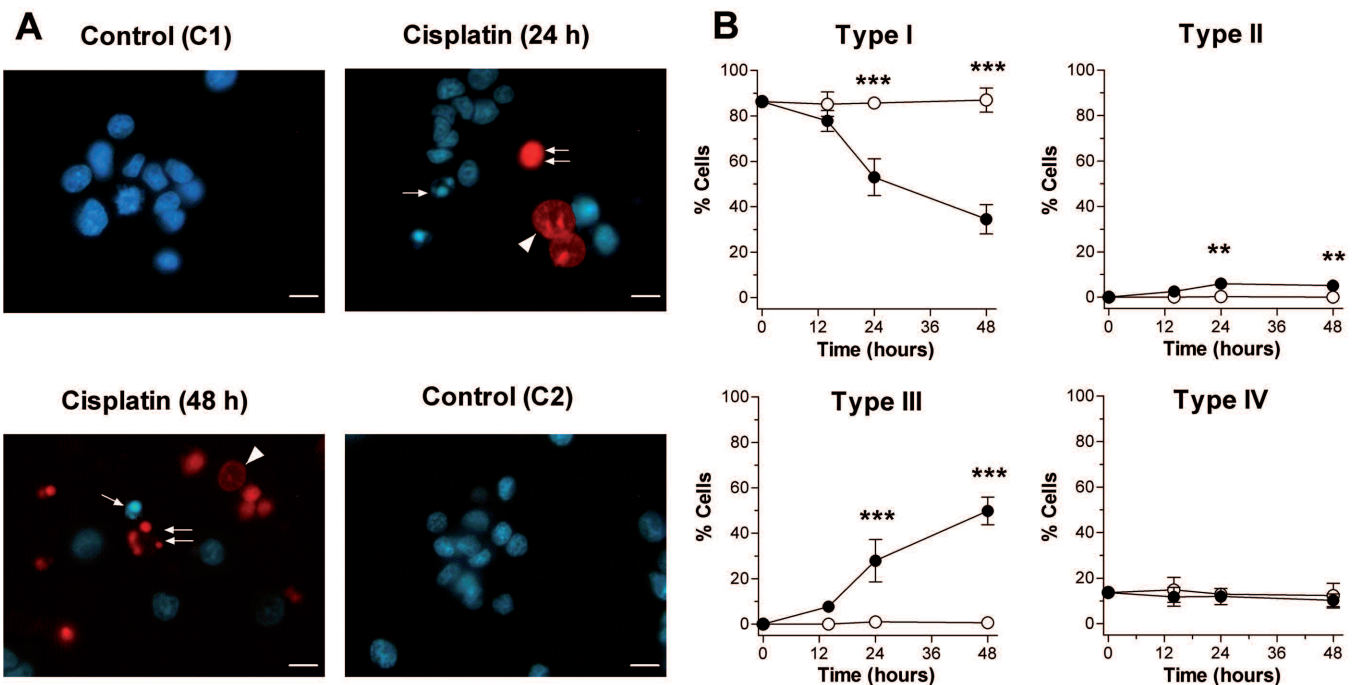


**Fig. 4.** Changes in nuclear morphology of PC12 cells exposed to cisplatin. Nuclear morphology was assessed with fluorescence microscopy in double-stained unfixed cells with the DNA-binding fluorochrome Hoechst 33342 (blue fluorescence) and propidium iodide (red fluorescence). **A.** Fluorescence micrographs of control, untreated and cisplatin-treated PC12 cells. On the basis of condensation and fragmentation of chromatin and uptake of propidium iodide, cells were classified in different phenotypes as type I, type II (arrow), type III (double arrow), and type IV (arrowhead). Scale bar: 10  $\mu$ m. **B.** Time-course of cell death phenotypes during cisplatin treatment. Data are presented as the mean  $\pm$  SEM of five independent experiments of triplicate (\*\*  $P < 0.01$ ; \*\*\*  $P < 0.001$ ).

## EPXMA of cisplatin-induced cell death

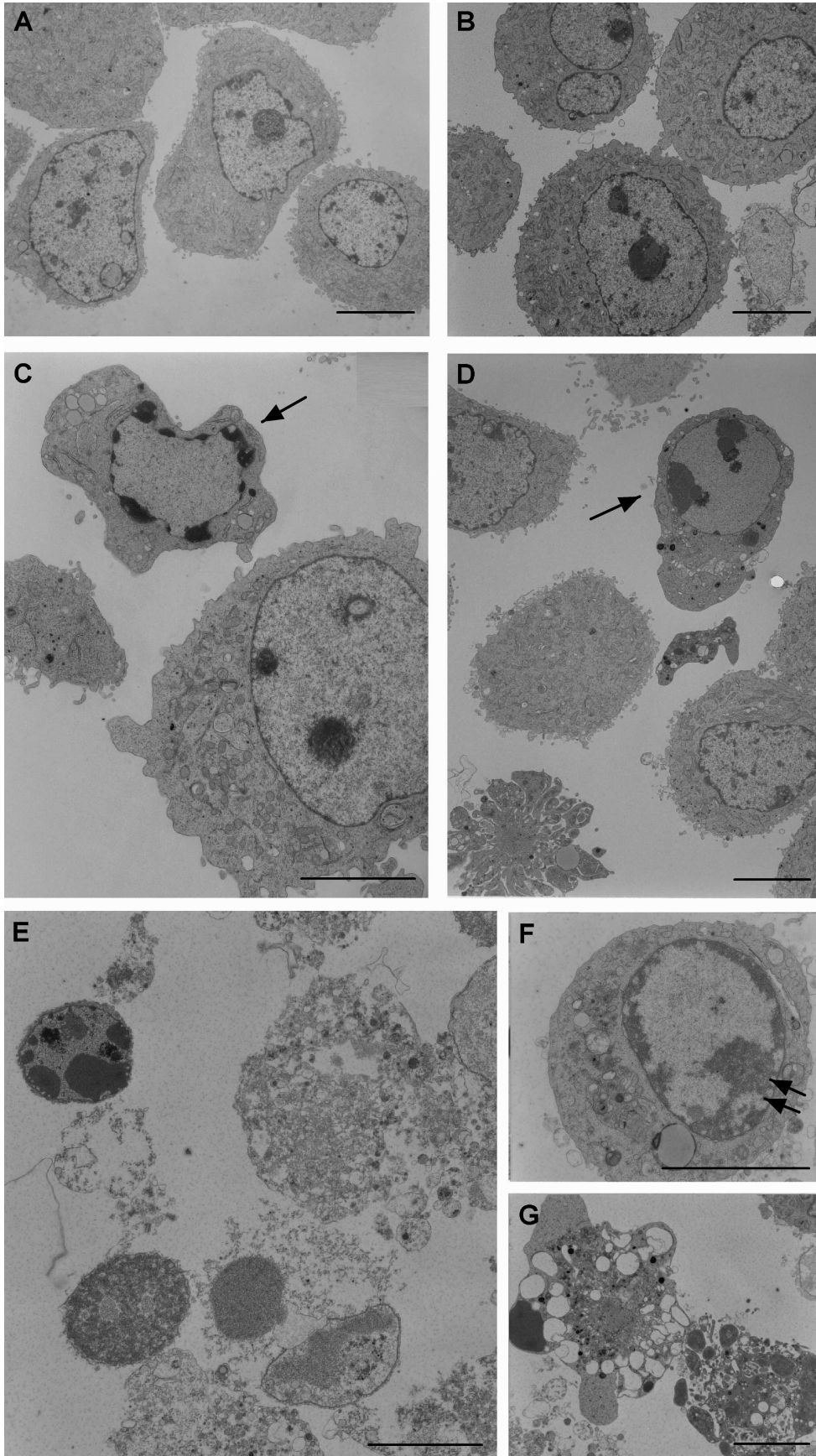


**Fig. 5.** Effects of cisplatin on cellular ultrastructure of PC12 cells examined with transmission electron microscopy. **A.** Normal control PC12 cells showed large nuclei, intact cellular organelles, and intact membranes. **B.** PC12 cells after 14 h of treatment with cisplatin. The cells showed no morphological alterations in ultrastructure. **C and D.** PC12 cells after 24 h of treatment with cisplatin. The cells showed morphological features typical of apoptosis (arrows), such as decreased size, condensed chromatin in the nucleus, and cytoplasmic condensation. Cells with no ultrastructural changes were also observed at this time. **E and F.** PC12 cells after 48 h of treatment with cisplatin. Cells displayed variable intermediate features of apoptosis and necrosis. The nucleus showed condensed chromatin (double arrows), a morphological feature typical of apoptosis. At this time necrotic changes such as cytoplasmic swelling (**F**), formation of vacuoles (**G**) and disruption of organelles and the plasma membrane were evident in association with apoptotic nuclei. Scale bar: 5  $\mu$ m.

that used EPXMA to determine elemental changes in apoptosis. Previously, we documented a significant decrease in K content and a significant increase in Na content in U937 cells in which apoptosis was induced by UV irradiation (Fernández-Segura et al., 1999; Arrebola et al., 2006). Another study with EPXMA reported similar alterations in Na and K content in association with DNA degradation studied by Tdt-mediated dUTP nick-end labeling (Skepper et al., 1999). Similar findings were reported in etoposide-induced apoptosis in prostate cancer cell lines (Salido et al., 2001, 2002). However, in these earlier studies with EPXMA the decrease in K and increase in Na were associated with a significant decrease in intracellular Cl content during apoptotic cell death. The simultaneous decrease in Cl and K content was related with loss of cell volume or cell shrinkage during apoptosis under normotonic conditions (Okada et al. 2001), and have been shown to be necessary for activation and assembly of the apoptotic machinery (Franco et al., 2006; Bortner and Cidlowski, 2007).

A number of studies have also documented an increase in Na and a decrease in K contents under ATP-depletion conditions (Buja et al., 1985; Jones et al., 1989) or progressive hypoxia (Thandroyen et al., 1992). In these cases intracellular Na and K alterations were associated with an increase in Cl content. These electrolyte alterations were related with cell swelling or the volume increase that accompanied necrotic cell death.

However, we reported that intracellular Cl content remained constant throughout the period of incubation with cisplatin. These data were different from the expected results for apoptosis or necrosis, and the reason for this observation is not clear. In this connection, Okada et al. (2004) reported that Cl<sup>-</sup> flux plays a dual role in the induction of different cell death mechanisms. The activation of volume Cl<sup>-</sup> channels and resulting decrease in intracellular Cl<sup>-</sup> concentration plays a cell-killing role in apoptosis (Ise et al., 2005). In contrast, dysfunction of these channels and the increase in cellular Cl<sup>-</sup> concentration are related with the persistence of cytoplasmic swelling during necrosis. Thus, the behavior of intracellular Cl content in cisplatin-treated PC12 cells was not consistent with either typical apoptosis or necrosis, and suggested a hybrid cell death mode.

Although P content might be suspected to vary during necrosis or apoptosis as a consequence of changes in the nucleus, our study demonstrated no significant time-course differences for this element. Roomans (2002) reported that the concentration of P remained the same as in undamaged cells, or decreased somewhat if structural damage was extensive during necrosis. In this study we show once again that there were no statistically significant differences in P content between untreated control cells and cisplatin-treated cells. The reason for the absence of any significant differences was because we analyzed only PC12 cells that did not show signs of extensive structural damage when examined in a scanning electron microscope in

secondary electron mode.

In this study, the EPXMA data were related to different morphological phenotypes identified on the basis of the cell's capacity to exclude vital fluorochromes, and changes in nuclear chromatin and other ultrastructural features of PC12 cells during cisplatin exposure. Here, we documented morphological evidence that cisplatin induced apoptosis in PC12 cells: microscopic examination of cells that had been double-labeled with Hoechst 33342 and PI revealed chromatin condensation and fragmentation in the presence of an intact plasma membrane (type II cells). This cell phenotype fulfills most of the criteria for apoptosis. In addition, these morphological features coexisted with a phenotype characterized by condensed chromatin and disruption of the plasma membrane (type III cells). Condensed or fragmented chromatin is a typical feature of apoptosis. In contrast, the inability to exclude vital stains is typical of necrosis. However, the mechanism that generates this hybrid cell phenotype is not clear.

Kaminski et al. (2004) suggested three origins for necrotic cells as a consequence of the absence of scavenging cells: 1) primarily necrotic cells that did not undergo apoptosis, 2) cells that became necrotic as a consequence of an unfinished apoptotic program, and 3) cells that became necrotic due to secondary necrosis following apoptosis. The capacity of therapeutic doses of cisplatin to induce primarily necrosis (type IV cells) was ruled out in the present study, since we found no differences between untreated and cisplatin-treated PC12 cells, and their proportions remained constant throughout the period of exposure to cisplatin. It is therefore possible that type III cells originated from an unfinished apoptotic program or from secondary necrosis. However, earlier studies have found that it is difficult to distinguish reliably between apoptotic, necrotic and mixed cells with fluorescence or confocal microscopy.

To obviate this difficulty, we used transmission electron microscopy techniques to distinguish between cell death modes, since these techniques are essential to determine the mode of cell death under given experimental conditions (Krysko et al., 2008). Our analysis of ultrastructural alterations confirmed that some PC12 cells exposed to therapeutic doses of cisplatin for 24 h showed the typical morphological phenotype of apoptosis. This phenotype coincided with type II cells identified by fluorescence microscopy. This proportion matched the proportion of cells with alterations in elemental content characteristic of apoptosis, i.e., an increase in intracellular Na and a decrease in intracellular Cl and K. However, we identified no cells with this characteristic profile for Na, Cl and K after 48 h of cisplatin treatment.

Analyses of individual cells with abnormal elemental contents at 48 h identified a large subset with increased intracellular Na, decreased K, and no change in Cl content. This microanalytical pattern was related with an ultrastructural phenotype characterized by intact

nuclei with condensed chromatin attached to the nuclear envelope, and accompanied by swollen but otherwise undamaged cytoplasm surrounded by an intact or disrupted plasma membrane.

Similar hybrid features of cell death were reported in previous electron microscopy studies of trophically deprived neurons (Peña and Pilar, 2000) and ouabain- and 4-aminopyridine-treated cortical neurons (Xiao et al., 2002; Wang et al., 2003). Electron microscopy studies with other insults and non-neuronal experimental models also described hybrid mechanisms of cell death with overlapping morphological features between apoptosis and necrosis (Simm et al., 1997; Formigli et al., 2000; Kaminski et al., 2004; Tardito et al., 2006). Segal-Bendirdjian and Jacquemin-Sablon (1995) reported similar morphological features in cisplatin-treated L1210 leukemic cells as a result of an unfinished apoptotic program. Thus the appearance of these particular phenotypes confirmed the coexistence of apoptotic and necrotic features in the same cell during exposure to therapeutic concentrations of cisplatin.

In conclusion, the inability of therapeutic doses of cisplatin to induce primarily necrosis, the inability of most treated cells to exclude vital stains, and the identification of cells with a variable phenotype combining morphological features of apoptosis and necrosis support the suggestion that increased Na, together with decreased K, and no changes in Cl content corresponded to cells undergoing a hybrid mechanism of cell death. This data supports the hypothesis that cisplatin-induced cell death is not always the result of the apoptotic cell death mechanism in PC12 cells. Finally, this comprises further support for the recommendation that data from EPXMA should be supplemented with the information provided by other methods that can provide additional information about the status of the cell.

---

*Acknowledgements.* The authors thank Ms Maria A. Robles for her expert technical assistance, K. Shashok for improving the use of English in the manuscript. This work was supported by grants from the Fondo de Investigaciones Sanitarias (FIS), Instituto de Salud Carlos III (Contract grant number PI 061836).

---

## References

- Andersson C. and Roomans G.M. (2002). Determination of chloride efflux by X-ray microanalysis versus MQAE-fluorescence. *Microsc. Res. Tech.* 59, 531-535.
- Arrebola F., Fernández-Segura E., Campos A., Crespo P.V., Skepper J.N. and Warley A. (2006). Changes in intracellular electrolyte concentrations during apoptosis induced by UV irradiation of human myeloblastic cells. *Am. J. Physiol. Cell. Physiol.* 290, C638-C649.
- Barros L.F., Hermosilla T. and Castro J. (2001). Necrotic volume increase and the early physiology of necrosis. *Comp. Biochem. Physiol. Part A* 130, 401-409.
- Bortner C.D. and Cidlowski J.A. (2007). Cell shrinkage and monovalent cation fluxes: role in apoptosis. *Arch. Biochem. Biophys.* 462, 176-188.
- Buja L.M., Hagler H.K., Parsons D., Chien K., Reynolds R.C. and Willerson J.T. (1985). Alterations of ultrastructure and elemental composition in cultured neonatal rat cardiac myocytes after metabolic inhibition with iodoacetic acid. *Lab. Invest.* 53, 397-411.
- Fernández-Segura E. and Warley A. (2008). Electron probe X-ray microanalysis for the study of cell physiology. *Methods Cell Biol.* 88, 19-43.
- Fernández-Segura E., Cañizares F.J., Cubero M.A., Warley A. and Campos A. (1999). Changes in elemental content during apoptotic cell death studied by electron probe X-ray microanalysis. *Exp. Cell. Res.* 253, 454-462.
- Fischer S.J., McDonald E.S., Gross L. and Windebank A.J. (2001). Alterations in cell cycle regulation underlie cisplatin induced apoptosis of dorsal root ganglion neurons in vivo. *Neurobiol. Dis.* 8, 1027-1035.
- Formigli L., Papucci L., Tani A., Schiavone N., Tempestini A., Orlandini G.E., Capaccioli S. and Orlandini S.Z. (2000). Aponecrosis: morphological and biochemical exploration of a syncytic process of cell death sharing apoptosis and necrosis. *J. Cell. Physiol.* 182, 41-49.
- Franco R., Bortner C.D. and Cidlowski J.A. (2006). Potential roles of electrogenic ion transport and plasma membrane depolarization in apoptosis. *J. Membr. Biol.* 209, 43-58.
- Gill J.S. and Windebank J. (1998). Cisplatin-induced apoptosis in rat dorsal ganglion neurons is associated with attempted entry into the cell cycle. *J. Clin. Invest.* 101, 2842-2850.
- González V.M., Fuertes M.A., Alonso C. and Pérez J.M. (2001). Is cisplatin-induced cell death always produced by apoptosis? *Mol. Pharmacol.* 59, 657-663.
- Ise T., Shimizu T., Lee E.L., Inoue H., Hohno K. and Okada Y. (2005). Roles of volume-sensitive Cl<sup>-</sup> channel in cisplatin-induced apoptosis in human epidermoid cancer cells. *J. Membr. Biol.* 205, 139-145.
- Jones R.L., Miller J.C., Hagler H.K., Chien K.R., Willerson J.T. and Buja L.M. (1989). Association between inhibition of arachidonic acid release and prevention of calcium loading during ATP depletion in cultured rat cardiac myocytes. *Am. J. Pathol.* 135, 541-556.
- Kaminski M., Niemczyk E., Masoka M., Karbowski M., Hallmann A., Kedzior J., Majczak A., Knap D., Nishizawa Y., Usukura J., Wozniak M., Limek J. and Wakabayashi T. (2004). The switch mechanism of the cell death mode from apoptosis to necrosis in menadione-treated human osteosarcoma cell line 143B cells. *Microsc. Res. Tech.* 64, 255-268.
- Krysko D.M., Berghe T.V., D'herde K. and Vandenabeele P. (2008). Apoptosis and necrosis: detection, discrimination and phagocytosis. *Methods* 44, 205-221.
- Lemasters J.J. (1999). Mechanisms of hepatic toxicity. V. Necrapoptosis and the mitochondrial permeability transition: shared pathways to necrosis and apoptosis. *Am. J. Physiol. (Gastrointest. Liver. Physiol.)* 39, 276, G1-G6.
- Maeno E., Takahashi N. and Okada Y. (2006). Dysfunction of regulatory volume increase is a key component of apoptosis. *FEBS Lett.* 580, 6513-6517.
- Maeno E., Ishizaki Y., Kanaseki T., Hazaña A. and Okada Y. (2000). Normotonic cell shrinkage because of disordered volume regulation is an early prerequisite to apoptosis. *Proc. Natl. Acad. Sci. USA* 97, 9487-9492.
- Okada Y., Maeno E., Shimizu T., Dezaki K., Wang J. and Morishima S. (2001). Receptor-mediated control of regulatory volume decrease

*EPXMA of cisplatin-induced cell death*

- (RVD) and apoptotic volume decrease (AVD). *J. Physiol.* 532, 3-16.
- Okada Y., Maeno E., Shimizu T., Manabe K., Mori S. and Nabekura T. (2004). Dual roles of plasmalemmal chloride channels in induction of cell death. *Pflugers. Arch.* 448, 287-295.
- Peña C. and Pilar G. (2000). Early morphologic alterations in trophically deprived neuronal death in vitro occur without alterations in cytoplasmic  $Ca^{2+}$ . *J. Comp. Neurol.* 424, 377-396.
- Pestell K.E., Hobbs S.M., Titley J.C., Kelland L.R. and Walton M.I. (2000). Effects of p53 status on sensitivity to platinum complex in a human ovarian cancer cell line. *Mol. Pharmacol.* 57, 50-511.
- Roomans G.M. (2002). X-ray microanalysis of epithelial cells in culture. *Methods Mol. Biol.* 188, 273-289.
- Salido M., Vilches J., Lopez A. and Roomans G.M. (2001). X-ray microanalysis of etoposide-induced apoptosis in the PC-3 prostatic cancer cell line. *Cell Biol. Int.* 25, 499-508.
- Salido M., Vilches J., Lopez A. and Roomans G.M. (2002). Neuropeptides bombesin and calcitonin inhibit apoptosis-related elemental changes in prostate carcinoma cell lines. *Cancer* 94, 368-377.
- Segal-Bendirdjian E. and Jacquemin-Sablon A. (1995). Cisplatin resistance in a murine leukemia cell line is associated with a defective apoptotic process. *Exp. Cell. Res.* 218, 201-212.
- Simm A., Bertsch G., Frank H., Zimmermann U. and Hoppe J. (1997). Cell death of AKR-2B fibroblasts after serum removal: a process between apoptosis and necrosis. *J. Cell. Sci.* 110, 819-828.
- Skepper J.N., Karydis I., Garnett M.R., Heigyi L., Hardwick S.J., Warley A, Mitchinson M.J. and Cary N.R.B. (1999). Changes in elemental concentrations are associated with early stages of apoptosis in human monocyte-macrophages exposed to oxidized low-density lipoprotein: an X-ray microanalytical study. *J. Pathol.* 188, 100-106.
- Spano A., Monaco G., Barni S. and Sciola L. (2008). Cisplatin treatment of NIH/3T3 cultures induces a form of autophagic death in polyploid cells. *Histol. Histopathol.* 23, 717-730.
- Sperandio S., De Belle I. and Bredesen D.E. (2000). An alternative, nonapoptotic form of programmed cell death. *Proc. Natl. Acad. Sci. USA* 97, 14376-14381.
- Tardito S., Bussolati O., Gaccioli F., Gatti R., Guizzardi S., Uggeri J., Marchio L., Lanfranchi M. and Franchi-Gazzola R. (2006). Non-apoptotic programmed cell death induced by a copper(II) complex in human fibrosarcoma cells. *Histochem. Cell. Biol.* 126, 473-82.
- Thandroyen F.T., Bellotto D., Katayama A., Hagler H.K., Willerson J.T. and Buja L.M. (1992). Subcellular electrolyte alterations during progressive hypoxia and following reoxygenation in isolated neonatal rat ventricular myocytes. *Cir. Res.* 71, 106-119.
- Warley A. (1997). X-ray microanalysis for biologists. Portland Press. London.
- Wang X.Q., Xiao A.Y., Yang A., Larose L., Wei L. and Yu S.P. (2003). Block of  $Na^+,K^+$ -ATPase and induction of hybrid death by 4-aminopyridine in cultured cortical neurons. *J. Pharmacol. Exp. Ther.* 305, 502-506.
- Xiao A.Y., Wei L., Xia S., Rothman S. and Yu S.P. (2002). Ionic mechanism of ouabain-induced concurrent apoptosis and necrosis in individual cultured cortical neurons. *J. Neurosci.* 22, 1350-1562.

Accepted September 28, 2010